Reactions of Laser-Ablated Y and La Atoms, Cations and Electrons with O_2. Infrared Spectra and Density Functional Calculations of the MO, MO^+, MO_2, MO_2^+, and MO_2^- Species in Solid Argon

Lester Andrews,* Mingfei Zhou, and George V. Chertihin

Department of Chemistry, University of Virginia, Charlottesville, Virginia 22901

Charles W. Bauschlicher, Jr.

Mail Stop 230-3, NASA Ames Research Center, Moffett Field, California 94035

Received: March 24, 1999; In Final Form: May 25, 1999

Laser-ablated Y and La condensed with O_2 in excess argon formed small metal oxides, cations, and anions, which were identified from isotopic substitution and density functional frequency calculations. In accord with gas phase thermochemistry, the OYO and OLaO molecules are more weakly bound than YO and LaO, on the basis of vibrational frequencies, and their symmetric stretching modes are unusually intense. The bent OYO^- and $OLaO^-$ anions, the cyclic $Y(O_2)^+$ and $La(O_2)^+$, and linear $OLaO^+$ cation isomers are characterized. The $(O_2)MO$ and MO_3 isomers are also observed.

Introduction

Despite the wide application of solid yttrium and lanthanum oxides in modern technology, especially in high-temperature superconductivity involving Y and La with Ba−Cu−O in perovskite oxide structures,[1,2] little is known about the simplest oxides of these metals. Furthermore, metal oxides serve as simple model systems for understanding bonding in transition metal compounds.[3] The YO and LaO diatomic molecules have been investigated in the gas phase by electronic and microwave spectroscopy[4−13] and in solid matrices by ESR and optical methods.[14,15] The gas phase thermochemistry of scandium, yttrium, and lanthanum dioxides found the dissociation energy of OM−O to be about a half of the diatomic M−O value,[16] which separates Sc from the early first row transition metals Ti and V where D(OM−O) ≈ 0.8−0.9 D(M−O). Such a small value of dissociation energy implies lower stretching vibrations and a less stable OScO molecule. Indeed, our recent investigation of the Sc+O_2 system found an antisymmetric vibration for a new OScO species at 722.5 cm^{-1}, which was first identified as the neutral molecule.[17,18] However, later experimental and theoretical work has shown that $(OScO)^-$ was observed instead of the neutral molecule.[19] Scandium and yttrium oxide anions have been investigated recently by photoelectron spectroscopy.[20]

Scandium and yttrium are special in transition metal chemistry; as with three electrons, Sc and Y fall between the alkaline earth metals Ca and Sr and the transition metals Ti and Zr. It is noteworthy that there are low lying configurations ($ns^2(n-1)$d and $ns(n-1)d^2$)[21] and the s and $(n-1)$d orbitals may simultaneously participate in bonding. In addition, calculations show that OScO is unusual in another respect: the symmetric stretching mode is substantially stronger and higher than the antisymmetric stretching mode. For the other bent first row dioxide molecules OTiO, OVO, OCrO, OMnO, and OFeO,[22−26] the antisymmetric stretching mode is by far the strongest infrared absorption. Here follows a study of laser-ablated Y and La atom reactions with O_2 which will be compared to the analogous Sc reactions.

Experimental Section

The technique for laser-ablation and matrix-infrared investigation has been described previously.[22−26] Yttrium and lanthanum targets were mounted on a rotating (1 rpm) stainless steel rod. The Nd:YAG laser fundamental (1064 nm, 10 Hz repetition rate, 10 ns pulse width) was focused on the target through a hole in CsI cryogenic (10 K) window. Laser power ranged from 1 to 10 mJ/pulse at the target. Metal atoms were co-deposited with 0.2−1.0% O_2 in argon (and isotopic modifications) for 1−2 h periods. Infrared spectra were recorded with 0.5 cm^{-1} resolution on a Nicolet 750 spectrometer. Matrix samples were temperature cycled, more spectra were collected, and selected samples were photolyzed by a medium-pressure mercury arc (Phillips, 175 W) with globe removed (240−580 nm).

Results

Infrared spectra of the Y+O_2 and La+O_2 systems in solid Ar and density functional calculations will be presented. These spectra contain many bands and show complicated behavior on photolysis and annealing. Figure 1 shows the spectra for Y+$^{16}O_2$, Figure 2 illustrates the effect of substitution with $^{16}O_2$+$^{16}O^{18}O$+$^{18}O_2$, and Table 1 lists the observed frequencies. Figures 3 and 4 illustrate the corresponding spectra for La and oxygen, and Table 2 gives the frequencies. These experiments were repeated with 0.1% CCl_4 added to serve as an electron trap, and anion reaction product bands were eliminated and cation products were enhanced relative to the corresponding neutral molecules, as observed in previous systems.[27] In particular O_4^+ and O_4^- bands at 1118.3 and 953.7 cm^{-1} are characteristic of these experiments,[28,29] and the latter is eliminated with CCl_4 present but the former remains. Figure 5 shows spectra from the Ar/O_2/CCl_4/Y sample. The results of isotopic substitution and photolysis and annealing behaviors for each band will be given with band assignments.

10.1021/jp991024z CCC: $18.00
Published on Web 08/03/1999

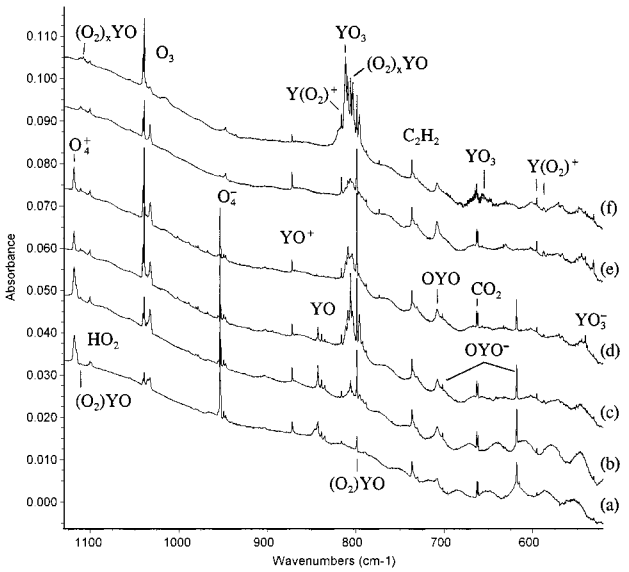

Figure 1. Infrared spectra in the 1130−520 cm^{-1} region for laser-ablated Y atoms, cations and electrons co-deposited with 0.5% O_2 in argon at 10 K. Sample (a) deposited for 1 h, (b) after 20 K annealing, (c) after 25 K annealing, (d) after $\lambda > 470$ nm photolysis, (e) after 240−580 nm photolysis, and (f) after 30 K annealing.

Calculations

Density functional theory calculations were performed on expected monoxide, dioxide, and trioxide products, including anions and cations, using the *Gaussian 94* program,[30] the BP86 functional,[31] the D95*, 6-31+G*, and 6-311+G(3d) basis sets for oxygen,[32] and the LanL2DZ basis set and pseudopotentials for yttrium and lanthanum.[33] Additional comparisons were made with the 6-311+G(2df) basis on O and LanL2DZ with an *f* function (0.192) on La using *Gaussian 98*. Calculated states, geometries, and vibrational frequencies for these molecules are compared in Tables 3, 4, and 5. Owing to computational cost considerations, the most extensive studies are carried out using the D95* basis set. Calibration calculations show that adding diffuse and additional polarization functions to the oxygen basis slightly reduces the calculated frequencies, but that the D95* basis set is sufficiently accurate to help interpret the spectra.

Discussion

The small metal oxide molecules, anions and cations will be identified from isotopic substitution and density functional calculations.

MO. The 843.1 and 796.7 cm^{-1} absorptions are assigned to YO and LaO in solid argon. These absorptions exhibited the diatomic 16/18 ratios (1.0505 and 1.0537) which are just below the harmonic diatomic ratios (1.0508 and 1.0540) owing to anharmonicity and gave doublets for the motion of a single O atom with scrambled isotopic precursor (Figures 2 and 4). These bands are red-shifted 12.1 and 11.6 cm^{-1} from the gas-phase 855.2 and 808.3 cm^{-1} fundamentals, respectively,[5] and are in excellent agreement with BP86 calculated (large basis) harmonic frequencies 860.1 and 783.0 cm^{-1} for the ground $^2\Sigma^+$ states. Part of the discrepancy is due to anharmonicity and part is due to matrix shift. Note that the calculation is high for Y and low for La. In like fashion, ScO was observed at 954.8 cm^{-1}, red-shifted 10.2 cm^{-1} from the gas-phase value, and 15.2 cm^{-1} below the BP86 frequency.[17]

MO^+. The 872.0 and 838.2 cm^{-1} absorptions are assigned to YO^+ and LaO^+ in solid argon. There are no gas-phase spectroscopic data for comparison. Again these bands exhibit the diatomic 16/18 ratios and doublets with scrambled isotopic oxygen. In the CCl_4-doped experiment with yttrium, the relative YO^+/YO band absorbance was increased 4× (Figure 5) compared to the regular undoped experiment (Figure 1) as CCl_4 captures electrons that might neutralize YO^+. The 838.2 cm^{-1} band was observed but CCl_4 masked the 796.7 cm^{-1} LaO absorption. Our BP86 calculations predict 916.6 and 833.3 cm^{-1} fundamentals for YO^+ and LaO^+ with $^1\Sigma^+$ ground states. The

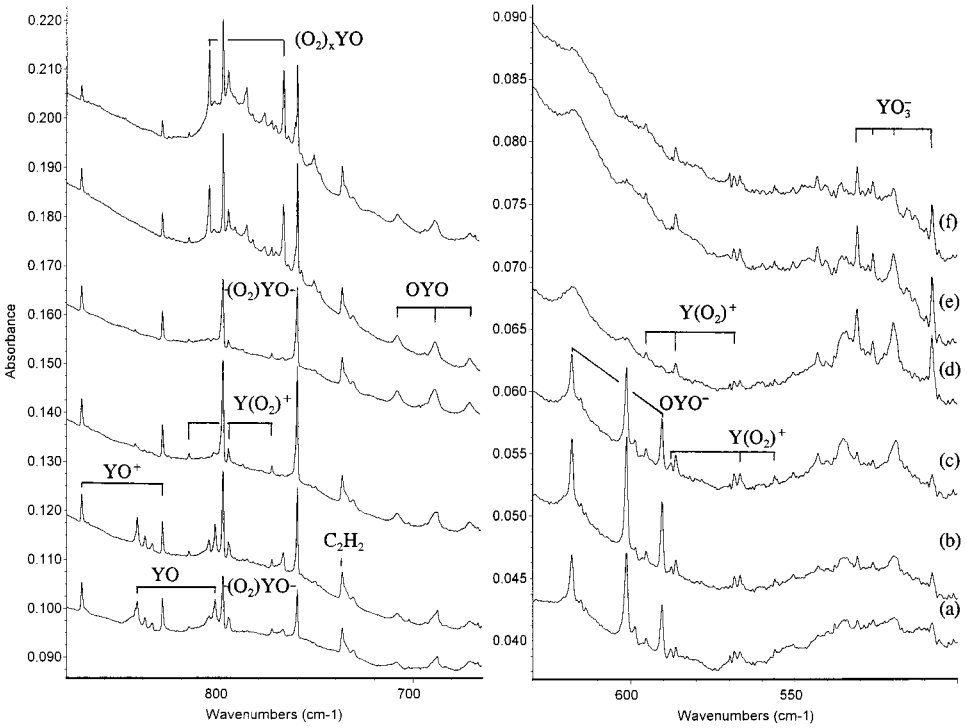

Figure 2. Infrared spectra in the 880−665 and 630−500 cm^{-1} regions for laser-ablated Y co-deposited with 0.8% statistical $^{16}O_2+^{16}O^{18}O+^{18}O_2$ in argon at 10 K. Sample (a) deposited for 1 h, (b) after 20 K annealing, (c) after $\lambda > 380$ nm photolysis, (d) after 240−580 nm photolysis, (e) after 25 K annealing, and (f) after 30 K annealing.

TABLE 1: Infrared Absorptions (cm^{-1}) from Reaction of Laser-Ablated Y Atoms with O_2 Molecules in Excess Argon at 10 K

$^{16}O_2$	$^{18}O_2$	$^{16}O_2+^{16}O^{18}O+^{18}O_2$	*R* (16/18)	assignment
1118.3	1055.7	1118.3,1102.3,1087.7,1084.8, 1071.1, 1055.7	1.0593	O_4^+
1111.1	1048.5	1111.1, 1080.4, 1048.5	1.0597	$(O_2)YO$
1107.8	1045.3	1107.8, 1077.0, 1045.3	1.0598	$(O_2)_xYO$
1039.5	982.2	1039.5, 1025.5, 1016.5, 1006.0, 991.5, 982.2	1.0583	O_3
1033.0	976.1	1033.0, 1019.3, 1010.4, 999.5, 985.4, 976.1	1.0583	O_3 site
953.7	901.6	953.7, 940.2, 928.2, 924.8, 914.1, 901.6	1.0578	O_4^-
872.0	830.0	872.0, 830.0	1.0506	YO^+
843.1	802.6	843.2, 802.6	1.0505	YO
839.1	798.9		1.0503	YO site
835.3	795.4		1.0502	YO site
816.3	773.1	816.3, 795.7, 773.1	1.0559	$Y(O_2)^+$ (ν_1)
811.5	766.7	811.5, 795.7, 789, 783, 776.9, 766.8	1.0584	YO_3
805.9	767.1	805.7, 767.1	1.0506	$(O_2)_xYO$
798.7	760.1	798.5, 760.1	1.0508	$(O_2)YO$
795.7	751.4	795.5, 786.3, 761, 751.4	1.0590	YO_3 site
773.5	731.5	773.3, 753.3, 731.6	1.0574	?
708.2	670.6	708.2, 688.5, 670.6	1.0561	OYO (ν_1)
702.0	666.4	702.0, 687.3, 666.4	1.0534	OYO^- (ν_1)
656.5	621.4	broad 650, 635, 622	1.0565	YO_3
618.0	590.5	618.0, 601.3, 590.5	1.0466	OYO^- (ν_3)
595.3	568.6	595.4, 586.3, 568.5	1.0470	$Y(O_2)^+$ (ν_2)
587.5	556.1	587.5, 566.7, 556.1	1.0565	$Y(O_2)^+$ (ν_3)
586.7	555.2	*	1.0567	$Y(O_2)^+$ site
546.2	520.4	546.2, 533.2, 520.4	1.0496	$(YO)_2$
530.8	507.6	530.8, 526.9, 519.6, 507.6	1.0457	YO_3^-
446.5	429.4	446.2, 442.9, 434.4, 429.6	1.0398	$Y(O_2)_2$

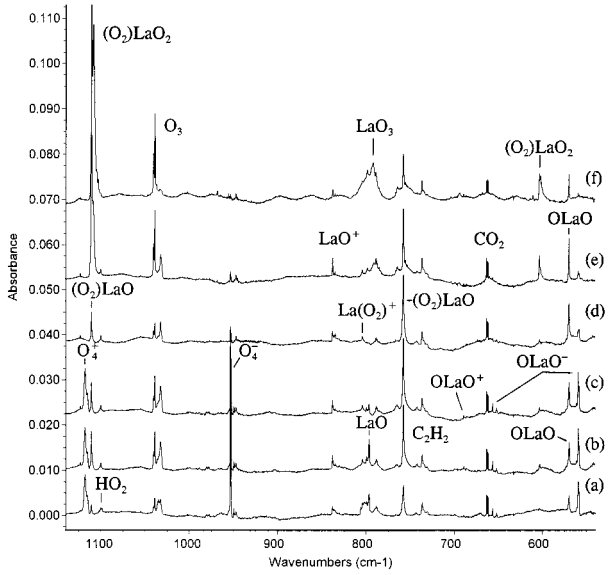

Figure 3. Infrared spectra in the 1140−540 cm^{-1} region for laser-ablated La atoms, cations and electrons co-deposited with 0.5% O_2 in argon at 10 K. Sample (a) deposited for 1 h, (b) after 20 K annealing, (c) after $\lambda > 470$ nm photolysis, (d) after 240−580 nm photolysis, (e) after 25 K annealing, and (f) after 30 K annealing.

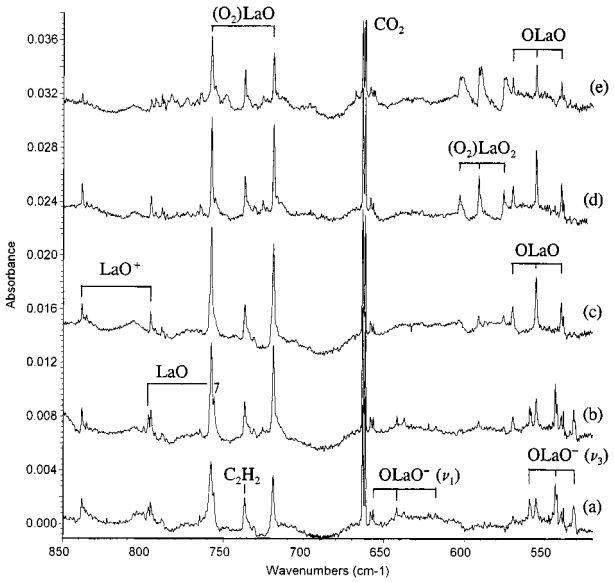

Figure 4. Infrared spectra in the 850−520 cm^{-1} region for laser-ablated La co-deposited with 0.8% statistical $^{16}O_2+^{16}O^{18}O+^{18}O_2$ in argon at 10 K. Sample (a) deposited for 1 h, (b) after 20 K annealing, (c) after 240−580 nm photolysis, (d) after 30 K annealing, and (e) after 35 K annealing.

difference between calculated and observed frequencies for YO^+ is larger (44.6 cm^{-1}) than found for YO (17.0 cm^{-1}) because of a larger anticipated matrix shift for the cation. Again the lanthanum calculated frequency is below the observed value. For La, there are many low-lying atomic states[21] derived from the $6s^15d^2$ occupation that can mix with the $^2D(6s^25d^1)$ ground state in the molecular systems. Apparently this mixing is not accurately accounted for in the DFT approach, so that the computed frequencies are smaller than observed, instead of larger, as is more typically the case.

The YO and YO^+ (LaO and LaO^+) species are made by the reaction of energetic laser-ablated Y atoms and Y^+ cations (La atoms and La^+ cations) with O_2 during the condensation process. There is a clear growth of YO^+ at the expense of YO on photolysis, and this is more dramatic with CCl_4 electron trap present (as was found for ScO^+ at the expense of ScO with CCl_4 present; note that ref 19 reassigns the blue site of ScO from ref 17 to the ScO^+ cation). We suspect that a sequential two-photon process through an intermediate YO* excited state may be involved, as has been proposed for the similar OScCO and $OScCO^+$ species.[34]

$(O_2)MO$. The 798.7 and 757.8 cm^{-1} absorptions are assigned to dioxygen complexes with the metal oxide. These bands also show diatomic 16/18 ratios and doublets with $^{16,18}O_2$ precursor and grow about 3× on annealing. For the La species, an associated 1123.4 cm^{-1} band is found with an O−O stretching 16/18 ratio (1.0596) and a triplet denoting two equivalent O atoms using $^{16,18}O_2$. For the Y species, the associated band is

TABLE 2: Infrared Absorptions (cm^{-1}) from Reaction of Laser-Ablated La Atoms with O_2 Molecules in Excess Argon at 10 K

$^{16}O_2$	$^{18}O_2$	$^{16}O_2+^{16}O^{18}O+^{18}O_2$	R (16/18)	assignment
1123.4	1060.2	1123.4, 1092.4, 1060.2	1.0596	$(O_2)LaO$
1118.3	1055.7	1118.3, 1102.3, 1087.7, 1084.9, 1071.2, 1055.9	1.0593	O_4^+
1111.1	1048.6	1111.0, 1080.6, 1048.5	1.0596	$(O_2)LaO_2$
1108.5	1046.4	1108.5, 1078.1, 1046.4	1.0593	$(O_2)LaO_2$ site
1039.4	982.2	1039.4, 1025.4, 1016.5, 1006.0, 991.5, 982.2	1.0582	O_3
1033.0	976.1	1033.0, 1019.3, 1010.4, 999.5, 985.4, 976.1	1.0583	O_3 site
953.7	901.6	953.7, 940.3, 928.2, 924.8, 914.1, 901.6	1.0578	O_4^-
838.2	795.4	838.2, 795.4	1.0538	LaO^+
804.0	758.7	804.0, 778.2, 759 sh	1.0597	$La(O_2)^+$
799.5				LaO site
796.7	756.1	796.7, 756.1	1.0537	LaO
792.2	748.1	sextet	1.0590	LaO_3
757.8	719.0	757.7, 719.0	1.0540	$(O_2)LaO$
689.3	657.9	689.4, 675.0, 657.9	1.0477	$OLaO^+$ (ν_3)
656.6	622.2	656.6, 641.9, 622.2	1.0553	$OLaO^-$ (ν_1)
651.9	617.5	651.8, 637.3, 617.5	1.0557	$OLaO^-$ (ν_1 site)
602.9	575.4	603.0, 591.0, 575.4	1.0478	$(O_2)LaO_2$ (ν_3)
601.8	574.3	601.8, 590.1, 574.3	1.0479	$(O_2)LaO_2$ (ν_3) site
569.8	539.5	569.8, 555.1, 539.4	1.0562	OLaO (ν_1)
559.2	531.8	559.2, 543.2, 531.8	1.0515	$OLaO^-$ (ν_3)
558.2	530.9	558.2, 541.2, 530.9	1.0514	$OLaO^-$ (ν_3) site

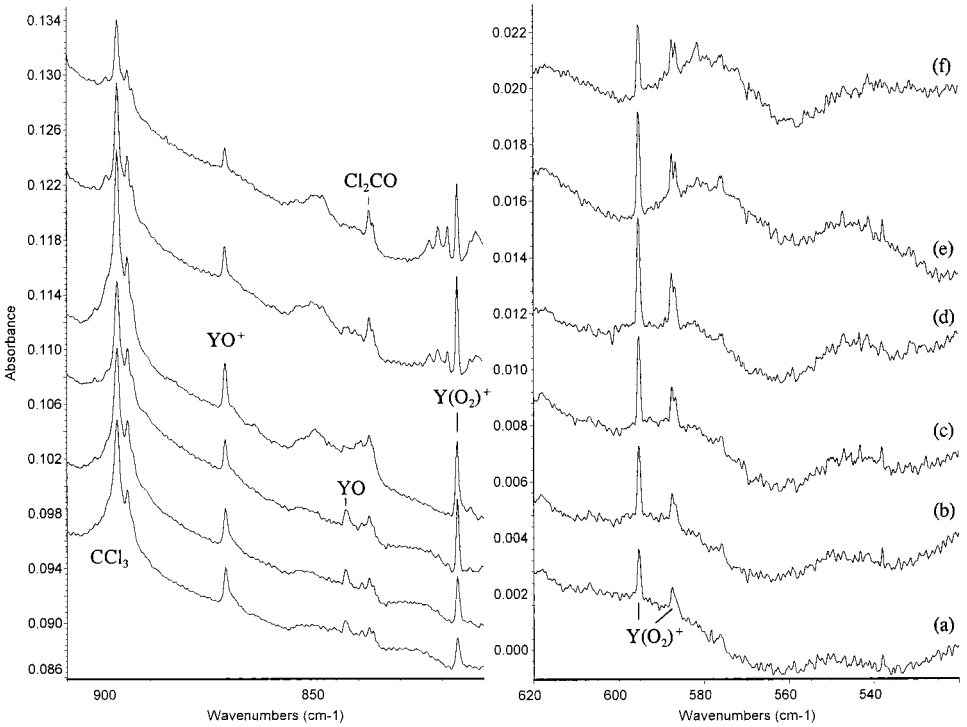

Figure 5. Infrared spectra in the 910−810 and 620−520 cm^{-1} regions for laser-ablated Y co-deposited with 0.5% O_2 and 0.1% CCl_4 in argon at 10 K. Sample (a) deposited for 1 h, (b) after 20 K annealing, (c) after 25 K annealing, (d) after 240−580 nm photolysis, (e) after 30 K annealing, and (f) after annealing to 35 K.

at 1111.1 cm^{-1} and a family of bands at and near 805.9 cm^{-1} appear on annealing along with bands at and near 1107.8 cm^{-1} for higher $(O_2)_xYO$ complexes that are apparently not formed for La. Our BP86 calculations predict these O_2 complexes to be red-shifted 55 and 37 cm^{-1}, respectively, from YO and LaO, and the observed bands are displaced 44 and 39 cm^{-1}, which is in very good agreement. Furthermore, the O−O stretching modes in the $(O_2)LaO$ and $(O_2)YO$ complexes are calculated to be 23 and 16 cm^{-1} above the observed values.

MO$^-$. The ScO^- anion fundamental was predicted at 910 cm^{-1} by BP86 calculations[19] and observed at 840 ± 60 cm^{-1} from a photodetachment hot band.[20] This anion could not be detected in the matrix infrared investigations.[17,19] Likewise, our BP86 calculation (large basis) predicts a 799.9 cm^{-1} YO^- fundamental, the photodetachment value is 740 ± 60 cm^{-1}, and there is no candidate in the present infrared spectrum. In addition, the BP86 energy for YO^- is 30 kcal/mol below YO and near the 31.3 kcal/mol experimental electron affinity.[20] Our BP86 calculation predicts LaO^- at 735.6 cm^{-1} and no absorption is observed in this region with the diatomic 16/18 ratio. Unfortunately, the MO^- absorptions may fall under bands because of the $(O_2)MO$ complexes.

OMO and OMO$^-$. The most interesting molecule here is the dioxide, where three valence electrons for M bonding two O atoms raises the theoretical question of molecular symmetry, and gas phase thermochemistry finds weak bonds.[16] Furthermore, the 722.5 cm^{-1} band first assigned to OScO has been reassigned to $OScO^-$, so these identifications are not straightforward.[17,19]

The BP86 calculations predict the anions to be normal dioxide molecules (isoelectronic to OZrO and OHfO)[22] with weak ν_1 (a_1) modes (70−100cm^{-1}) higher than the very strong ν_3 (b_1)

TABLE 3: Calculated (BP86/D95* or 6-311+G(3d)/LanL2DZ) States, Relative Energies (kcal/mol), Bond Lengths, Vibrational Frequencies (cm^{-1}), and Intensities (km/mol) for YO, YO^+,YO^-, LaO, LaO^+, and LaO^-

molecule	energy	length (Å)	freq(int)
YO ($^2\Sigma^+$)[a]	0	1.823	873.1(108)
YO^+ ($^1\Sigma^+$)[a]	145	1.786	925.2(113)
YO^- ($^1\Sigma^+$)[a]	−30	1.864	817.9(132)
LaO ($^2\Sigma^+$)[a]	0	1.973	784.7(109)
LaO^+ ($^1\Sigma^+$)[a]	130	1.939	826.3(98)
LaO^- ($^1\Sigma^+$)[a]	−26	2.010	743.2(127)
YO ($^2\Sigma^+$)[b]	0	1.838	860.1(143)
YO ($^2\Delta$)[b]	+33	1.861	796.8(131)
YO ($^2\Pi$)[b]	+42	1.850	817.2(189)
YO^+ ($^1\Sigma^+$)[b]	+146	1.797	916.6(121)
YO^- ($^1\Sigma^+$)[b]	−30	1.877	799.9(193)
LaO ($^2\Sigma^+$)[b]	0	1.977	783.0(160)
LaO^+ ($^1\Sigma^+$)[b]	+131	1.938	833.3(111)
LaO^- ($^1\Sigma^+$)[b]	−26	2.013	735.6(206)
LaO ($^2\_\Sigma^+$)[c]	0	1.957	770.4(162)
LaO^+($^1\Sigma^+$)[c]	+131	1.916	817.6(107)

[a] Small D95* basis on O. [b] Large 6-311+G(3d) basis on O. [c] 6-311+G(2df) basis on O and LanL2DZ with *f* on La.

modes; however, the neutral molecules are very unusual with ν_1 (a_1) predicted substantially higher (180−205 cm^{-1}) and stronger (>8× for OYO) than ν_3 (b_1). The same relationship has been calculated for the scandium species.[17−19]

Three bands in each metal experiment are due to these two species. In the Y case, a 708.2 cm^{-1} band grows on first annealing and full-arc photolysis and then gives way on higher annealing. This band is reduced but still observed with CCl_4 doping. Sharp 702.0 and 618.0 cm^{-1} bands increase (40%) on 20 K annealing, decrease (15%) on $\lambda > 470$ photolysis, disappear on full-arc irradiation, and are not observed with CCl_4 doping as is the case with the 953.7 cm^{-1} O_4^- band. These bands appear as doublets in $^{16}O_2$+$^{18}O_2$ experiments, which shows that one O_2 molecule is involved, and 1/2/1 triplets with unshifted pure isotopic components are formed using $^{16}O_2$+$^{16}O^{18}O$+$^{18}O_2$ (Figure 2), which demonstrates the involvement of two equivalent O atoms in these modes.

The BP86 calculations confirm assignment of the sharp bands at 702.0 and 618.6 cm^{-1} to ν_1 (a_1) and ν_3 (b_1) of OYO^- predicted at 715.4 and 612.6 cm^{-1}, respectively, with 1 to 50 relative intensity (1 to 10 observed). The observed 16/18 ratios (1.0534 and 1.0466) further characterize these symmetric and antisymmetric modes and agree well with the calculated 16/18 frequency ratios (1.0527 and 1.0481). The calculated valence angle (109.9°) is in accord with the angle upper limit[35] prediction (123°) from the 16/18 ratio for ν_3 (b_1). Finally, the absence of these bands, and the O_4^- absorption, with added CCl_4 electron trap[27] provides strong experimental support for the OYO^- anion identification.

The full-arc photolysis that destroys OYO^- increases the broader 708.2 cm^{-1} band, which is also due to a species with two equivalent oxygen atoms. The observed 16/18 ratio (1.0561) indicates a symmetric M−O stretching mode, and the BP86 calculation predicts ν_1 (a_1) of bent OYO at 704.7 cm^{-1}. The weaker ν_3 (b_1) mode is predicted at 499.0 cm^{-1} with 4% of the ν_1 mode intensity and cannot be observed in the noise level. Accordingly, the 708.2 cm^{-1} band is assigned to ν_1 (a_1) of the OYO dioxide molecule, which is in agreement with the photoelectron band spacing (640 ± 80 cm^{-1}) within experimental error.[20] Despite multiconfigurational character, we have shown for OScO that DFT can treat such systems.[18,19]

The substantial growth of OYO on annealing suggests that the insertion reaction 1 proceeds without activation energy. Relaxation by the matrix is needed to stabilize OYO, otherwise decomposition to YO will result. During co-deposition ablated electrons are captured by OYO to form OYO^-, reaction 2. The substantial electron affinity of OYO (46.1 kcal/mol)[20] is in accord with the failure to efficiently photodetach OYO^- with $\lambda > 470$ nm photolysis. The growth of OYO on full-arc photolysis is due to this photodetachment process, reaction 3. It is also possible for OYO^- to arise from reaction 4 as O_2^- is involved in reaction 5 to form O_4^-. Finally, the present BP86 calculations find OYO^- more stable than OYO by 45 kcal/mol (large basis), which is near the experimental electron affinity.[20]

$$Y + O_2 \rightarrow (OYO)^* \xrightarrow{\text{relax}} OYO \quad (1a)$$

$$\xrightarrow{\text{decompose}} O + YO \quad (1b)$$

$$OYO + e^- \rightarrow OYO^- \quad (2)$$

$$OYO^- + h\nu \rightarrow OYO + e^- \quad (3)$$

$$Y + O_2^- \rightarrow OYO^- \quad (4)$$

$$O_2 + O_2^- \rightarrow O_4^- \quad (5)$$

In the La case, a sharp 569.8 cm^{-1} band grows on 20 K annealing (2×), on $\lambda > 470$ nm photolysis (+20%), on full-arc photolysis (+33%), and on 25 K annealing (+20%), while sharp 656.6 and 559.2 cm^{-1} bands increase less on 20 K annealing (+20%) and decrease on $\lambda > 470$ nm (10%), full-arc (80%) photolyses, and 25 K annealing (30%), (Figure 3). Doping with CCl_4 eliminates the 656.6 and 559.2 cm^{-1} bands while the 569.8 cm^{-1} band is reduced (0.5×) but behaves the same as described above. These bands exhibit the same mixed isotopic behavior (Table 2) as the analogous Y bands, so one O_2 molecule with equivalent O atoms is involved in these reaction products, which are identified as bent OLaO and $OLaO^-$. The only difference is that the BP86 calculated frequencies do not fit as well for the La species, which is probably caused by other low energy configurations. The calculation predicts a 105.4° valence angle for $OLaO^-$, which is in accord with the upper limit estimate (116°) from the observed 16/18 ν_3 (b_1) frequency ratio.[35] Reactions 1−4 can also be written for lanthanum.

$M(O_2)^+$. In contrast to the neutral dioxide, the most stable cation isomer is the cyclic form, and the $Sc(O_2)^+$ cation has recently been identified by three stretching fundamentals at 892.9, 641.1, and 624.8 cm^{-1}, which are modeled extremely well by DFT frequency calculations.[19] The sharp Y product bands at 816.3, 595.3, and 587.5 cm^{-1} are favored 2× on doping with CCl_4 to trap electrons and are accurately characterized by the BP86 predictions of 870.4, 588.0, and 587.9 cm^{-1} bands with 16/18 ratios 1.0571, 1.0474, and 1.0578, respectively, for the cyclic $Y(O_2)^+$ cation. This molecular cation is made by direct reaction of Y^+ cation with O_2 followed by matrix relaxation. The YO^+ cation discussed earlier is probably formed from this reaction without efficient matrix relaxation.

$$Y^+ + O_2 \rightarrow Y(O_2)^+ \quad (6)$$

The sharp 804.0 cm^{-1} band for La clearly shows different annealing behavior than LaO, and the $^{18}O_2$ counterpart at 758.7 cm^{-1} defines a different motion (16/18 ratio 1.0597). The band gives a triplet with $^{16,18}O_2$ expected for two equivalent O atoms. Unfortunately the band was only evidenced by a shoulder on the blue wing of the CCl_4 absorption. The sharp 804.0 cm^{-1} band is assigned to the O−O stretching mode of $La(O_2)^+$ calculated by BP86 at 860.2 cm^{-1} with 16/18 ratio 1.0595. Our

TABLE 4: Calculated (BP86/D95*/LanL2DZ) States, Relative Energies (kcal/mol), Geometries, Isotopic Vibrational Frequencies (cm^{-1}), and Intensities (km/mol) for YO_2 and LaO_2 Molecules, Cations, and Anions and Comparisons with Larger Basis Sets

molecule	energy	bond lengths, angles	ν_1	ν_2	ν_3
$OYO(^2B_2)$	0	1.927 Å, 115.3°	704.7(53)	111.8(25)	499.0(2)
18−89−18			668.0(49)	106.5(22)	476.3(2)
R(16/18)			1.0549	1.0498	1.0477
$Y(O_2)(^2A_1)$	28	2.016 Å, 1.503 Å, 43.8°	849.6(51)	568.6(21)	541.0(3)
89−18−18			802.8(47)	543.6(18)	511.4(3)
R(16/18)			1.0583	1.0460	1.0579
$OYO^-(^1A_1)$	−41	1.948 Å, 109.9°	715.4(4)	215.8(0)	612.6(206)
18−89−18			679.6(4)	205.2(0)	584.5(186)
R(16/18)			1.0527	1.0517	1.0481
$Y(O_2)^+(^1A_1)$	175	1.977 Å, 1.500 Å, 44.6°	870.4(54)	588.0(21)	587.9(16)
89−18−18			823.4(50)	561.4(20)	555.8(16)
R(16/18)			1.0571	1.0474	1.0578
$OYO^+(^3B_2)$	215	1.980 Å, 125.0°	547.6(30)	109.2(30)	453.1(37)
$OYO^+(^1\Sigma_g^+)$	223	1.848 Å, 180°	656.1(0)	149.3(42)	779.0(41)
18−89−18			618.5(0)	143.1(40)	746.4(39)
R(16/18)			1.0608	1.0433	1.0437
$OYO(^2B_2)^a$		1.939 Å, 116.3°	682.2(60)	103.0(29)	482.4(4)
$OYO^+(^3B_2)^a$	217	1.993 Å, 125.7°	541.3(31)	113.1(32)	446.7(36)
$OYO^-(^1A_1)^a$	−46	1.962 Å, 111.0°	701.3(23)	213.2(0)	608.0(324)
$OYO(^2B_2)^b$	0	1.941 Å, 123.2°	680.1(47)	114.2(35)	502.8(6)
$OYO^-(^1A_1)^b$	−45	1.965 Å, 112.8°	701.5(21)	194.2(0)	608.1(323)
$OLaO(^2B_2)$	0	2.078 Å, 111.8°	640.7(57)	142.7(20)	440.2(1)
18−139−18			606.3(52)	135.6(18)	418.5(1)
R(16/18)			1.0567	1.0524	1.0519
$La(O_2)(^2A_1)$	32	2.185 Å, 1.494 Å, 40.0°	841.7(55)	504.4(26)	497.7(9)
139−18−18			794.2(49)	480.6(24)	469.9(8)
R(16/18)			1.0598	1.0495	1.0592
$OLaO^-(^1A_1)$	−40	2.080 Å, 105.4°	655.6(13)	223.2(0.1)	587.3(172)
18−139−18			621.4(11)	211.7(0.1)	558.1(155)
R(16/18)			1.0550	1.0543	1.0523
$La(O_2)^+(^1A_1)$	166	2.149 Å, 1.488 Å, 40.5°	860.2(49)	524.0(19)	533.4(12)
139−18−18			811.9(45)	499.1(18)	503.7(12)
R(16/18)			1.0595	1.0499	1.0590
$OLaO^+(^3B_2)$	205	2.125 Å, 115.6°	426.8(18)	91.9(16)	473.3(35)
$OLaO^+(^1\Sigma_g^+)$	206	2.125 Å, 180°	621.6(0)	173.1(31)	728.6(52)
18−139−18			586.0(0)	165.1(29)	694.8(49)
R(16/18)			1.0608	1.0485	1.0486
$OLaO(^2B_2)^a$	0	2.084 Å, 112.8°	621.5(67)	133.0(23)	423.0(5)
$La(O_2)(^2A_1)^a$	32	2.189 Å, 1.500 Å, 40.0°	826.3(67)	503.0(37)	493.8(12)
$OLaO^-(^1A_1)^a$	−44	2.093 Å, 106.1°	638.9(69)	218.4(0.1)	571.3(290)
$OLaO^+(^1\Sigma_g^+)^a$	208	1.982 Å, 180°	613.8(0)	161.6(31)	725.1(61)
$OLaO(^2B_2)^b$	0	2.082 Å, 115.8°	626.8(61)	125.4(23)	437.0(6)
$OLaO^-(^1A_1)^b$	−43	2.090 Å, 107.0°	647.7(72)	216.2(0)	579.6(288)
$OLaO^+(^1\Sigma_g^+)^b$	204	1.975 Å, 180°	594.0(0)	177.7(30)	714.1(51)
$OLaO(^2B_2)^c$	0	2.066 Å, 117.1°	619.5(55)	127.9(25)	431.5(7)
$OLaO^-(^1A_1)^c$	−44	2.078 Å, 107.9°	644.8(64)	216.7(0.1)	570.4(278)
$OLaO^+(^1\Sigma_g^+)^c$	+205	1.969 Å, 180°	616.7(0)	168.4(35)	716.2(55)
$OLaO^+(^3B_2)^c$	+206	2.102 Å, 115.5°	430.4(34)	93.4(15)	419.4(23)

[a] The 6-31+G* basis on O. [b] The 6-311+G(3d) basis on O. [c] The 6-311+G(2df) basis on O, LanL2DZ with f for La.

TABLE 5: Calculated (BP86/D95*/LanL2DZ) States, Relative Energies (kcal/mol), Geometries, Vibrational Frequencies (cm^{-1}), and Intensities (km/mol) for YO_3 and LaO_3 Species

molecule	energy	geometry	frequency (intensity)
$(O_2)YO$ ($^2A''$)	0	Y−O:1.845 Å, O−O:1.355 Å ∠OYO:34.9°, ∠O−Y−O_2:110.0°	127(46), 818(100), 399(5), 398(39), 160(11), 155(19)
YO_3^- (D_{3h})	−32	Y−O:2.008 Å ∠OYO:120.0°	576(0), 538(2 × 1), 175(2 × 18), 129(107)
YO_3 ($^2A'$)	56	Y−O:2.093 Å, O−O:1.495 Å ∠OOO:107.2°, ∠OYO:70.2 dYOO:129.0°	843(33), 648(48), 602(29), 415(16), 381(1), 262(1)
(O_2) LaO ($^2A''$)		La−O:1.990, O−O 1.347 Å ∠OLaO:31.9°, ∠O−La−O_2:105.6°	1147(51), 748(110), 361(4), 353(36), 150(6), 110(16)

BP86 calculations predict $La(O_2^+)$ 10.2 cm^{-1} below $Y(O_2)^+$ and experiments find the strong O−O modes of these cations 12.3 cm^{-1} apart.

$OLaO^+$. The open cations are calculated to be on the order of 40 kcal/mol above the corresponding cyclic $M(O_2)^+$ cations and there is no evidence for such a species with Sc and Y. The bent $^3B_2$ and linear $^1\Sigma_g^+$ forms of OYO^+ are 39.7 and 47.8 kcal/mol higher than cyclic $Y(O_2)^+$ and are not observed in these experiments. The $^3B_2$ and $^1\Sigma_g^+$ states of $OLaO^+$ are 38.6 and 40.0 kcal above the cyclic $^1A_1$ state, but the linear cation is predicted to absorb very strongly at 728.6 cm^{-1}. A very weak 689.3 cm^{-1} band is favored 3× in absolute intensity and 5× relative to OLaO with added CCl_4 and shows a 1/2/1 triplet with $^{16,18}O_2$ reagent and the 16/18 ratio 1.0477. The harmonic antisymmetric stretching mode for linear O−La−O exhibits a 1.0486 ratio. This observed value is appropriate for the linear structure with anharmonicity taken into account. Note asymmetry in the triplet 689.4−675.0−657.9 cm^{-1}; displacement of the central $^{16}O-La-^{18}O$ component 1.3 cm^{-1} above the median indicates that the symmetric counterpart is lower as predicted

by the calculation for $^1\Sigma_g^+$ $OLaO^+$ in contrast to calculations for OLaO and $OLaO^-$. Accordingly, the sharp 689.3 cm^{-1} band is assigned to linear $OLaO^+$.

It is perhaps surprising that the linear $OLaO^+$ cation isomer is observed here in addition to the 40 kcal/mol more stable cyclic $La(O_2)^+$ cation. In the presence of CCl_4, which allows the survival of more La^+ during deposition, annealing to 25 K increases the $OLaO^+$ absorption (2×) with little change in the $La(O_2)^+$ peak. Apparently, the La^+ reaction with O_2 is sufficiently exothermic to access both states. Clearly, there will be a barrier for the linear cation to form the cyclic cation once the linear cation is trapped in the matrix.

$$La^+ + O_2 \rightarrow La(O_2)^+ \text{ and } OLaO^+ \quad (7)$$

YO_3^-. A weak 530.8 cm^{-1} band *increases* 5× on full-arc photolysis at the expense of the strong 798.7 cm^{-1} $(O_2)YO$ absorption while OYO^- *decreases* and OYO *increases* (Figure 1). In gas-phase photodetachment studies, YO_3^- has a broad 3 eV binding energy feature and is therefore much more difficult to photodetach than OYO^- (the OYO electron affinity is 2.00 eV).[20] The 530.8 cm^{-1} band exhibits a 1.0457 isotopic 16/18 ratio, which denotes an antisymmetric Y−O stretching mode and a O−Y−O angle slightly less than the 123° value estimated for $O-Y-O^-$ from the 16/18 ratio. The $^{16,18}O_2$ isotopic spectrum shows two strong pure isotopic bands with two weaker intermediate mixed isotopic components, which is the pattern expected for the doubly degenerate stretching mode of a trigonal species where the mixed isotopic molecules also contribute to the pure isotopic bands.[24,37] Accordingly, the 530.8 cm^{-1} band is assigned to YO_3^-. A similar band has been observed at 817.1 cm^{-1} for NbO_3^-.[38]

Our BP86 calculations find a stable trigonal planar YO_3^- anion with degenerate mode at 538 cm^{-1}, which is in excellent agreement with the observed spectrum. The calculated bond length (2.008 Å) is slightly longer than in OYO^- (1.948 Å).

The photodetachment spectrum was assigned to the ozonide isomer YO_3.[20] This molecule probably has a cyclic structure with the O_3 part giving the strong antisymmetric O−O−O stretching mode discussed below, which is not the mode observed for YO_3^- at 530.8 cm^{-1}. Photodetachment from YO_3^- (D_{3h}) probably gives a trigonal radical, which forms an O−O bond and lowers symmetry to the more stable $(O_2)YO$ species.

MO_3. A strong 804.0 cm^{-1} band appeared on annealing in the Sc experiments and showed the 16/18 ratio (1.0590) and the mixed isotopic spectrum for a trioxygen species. The band at 811.5 cm^{-1} with Y increases markedly on annealing, decreases on photolysis, and shifts to 766.7 cm^{-1} using $^{18}O_2$ (1.0584 ratio). The $^{16}O_2+^{18}O_2$ spectrum gave a 811.5, 795.7, 776.9, 766.8 cm^{-1} quartet, and the scrambled isotopic precursor produced the sextet listed in Table 1. This MO_3 isomer is made by the reaction of MO and O_2 at the oxide site on annealing, which is much more important for the alkaline earth metals that form ionic ozonides, or by reaction of Y with O_3, which is formed on deposition.[36] However, the near agreement of the "ionic" $M^+O_3^-$ ozonide band near 800 cm^{-1}, which is the antisymmetric ν_3 (b_1) O_3^- fundamental, and the present 811.5 cm^{-1} band, which is due to the symmetric O−O−O stretching mode of the O_3 subunit in the nonplanar "covalent" YO_3 ring, is misleading. BP86 calculations show that ScO_3 and YO_3 are nonplanar ring structures (not ionic ozonides) and predict the two strongest (symmetric and antisymmetric O−O−O) stretching modes at 843 and 648 cm^{-1} (Table 5). In addition, a weaker 656.5 cm^{-1} band is probably due to the antisymmetric O−O−O stretching mode of YO_3. Interestingly, strong ozonide type absorptions were observed only for Cu and Zn among the first row transition metals.[39,40] The weak 792.2 cm^{-1} absorption in La experiments is counterpart for this MO_3 ring species. In contrast to lanthanum, the major stable annealing product is O_2 perturbed OLaO.

MO_4 Species. With scandium, a strong 552.6 cm^{-1} band appeared on annealing and exhibited a low (1.0306) 16/18 isotopic ratio consistent with the antisymmetric vibration of Sc between two O_2 units and an appropriate mixed isotopic pattern for the bisdioxygen species. This band was assigned to D_{2d} (O_2)-$Sc(O_2)$ with the support of DFT frequency calculations.[17] A similar band appears at 446.5 cm^{-1} on annealing in Y experiments and does not change on photolysis. This band shows a low (1.0398) 16/18 ratio suggesting the vibration of Y between two O_2 units. The $^{16}O_2+^{18}O_2$ experiment gave a triplet absorption at 446.5, 443.0, 429.4 cm^{-1}, and the scrambled isotopic sample gave the broadened multiplet listed in Table 2. The 446.5 cm^{-1} band is appropriate for assignment to $(O_2)Y(O_2)$. If such a species is formed with La, it must absorb below the 410 cm^{-1} low-frequency limit of our spectrometer.

However, with La sharp bands at 1111.1 and 602.9 cm^{-1} increase markedly (7×) on 25 K annealing and are not affected by photolysis. Both bands show 1/2/1 triplets for vibrations of two equivalent O atoms, but the upper band exhibits the 16/18 isotopic ratio 1.0596 for a pure O−O stretching mode and the lower band the 1.0478 ratio for the antisymmetric O−La−O stretch of a linear subunit. These two modes characterize a side-bound O_2 complex to a linear O−La−O species. Such complexes have been observed[23−26,38] for VO_2, CrO_2, MnO_2, FeO_2, and particularly[41] for RhO_2 and IrO_2, but we found no evidence for such a species with YO_2.

Other Absorptions. The weak band at 546.6 cm^{-1} that grows on annealing is favored by higher laser power and gives an appropriate 16/18 isotopic ratio and mixed isotopic spectrum for $(YO)_2$ dimer. Finally, the sharp 773.5 cm^{-1} band increases on photolysis and is due to a symmetric motion from the high 16/18 ratio, but the small secondary isotopic shifts suggest the involvement of more than one O_2 molecule. Without more information, this absorber cannot be identified.

Conclusions

Laser-ablated Y and La condensed with O_2 in excess argon formed the metal oxides, cations, and anions, which were identified from isotopic substitution and density functional frequency calculations. This work and previous scandium[17,19] and lanthanide[42] metal investigations clearly show that laser ablation produces metal atoms, metal cations, and electrons and that reaction products involving all three can be trapped in the matrix for infrared spectroscopic study. The simple addition of CCl_4 as a chemical electron trap removes electrons and eliminates molecular anion product absorptions and accordingly enhances cation reaction product bands.[27] The YO and LaO molecules are observed 12.1 and 11.6 cm^{-1} red-shifted from gas-phase values,[5] and the matrix absorptions for YO^+ and LaO^+ predict gas-phase fundamentals near 900 and 870 cm^{-1}, respectively.

Gas phase thermochemical studies[16] have predicted weak bonds in the O−M−O molecules (M = Sc, Y, La) and we find low ν_1 (a_1) frequencies. DFT calculations show that these Group 3 dioxide molecules are unique among transition metal dioxides in that the symmetric stretching mode is substantially higher (41% for OYO) and markedly stronger (25× for OYO) than the antisymmetric stretching mode.

The OMO^- anions are stable as the isoelectronic high-temperature OTiO, OZrO and OHfO molecules indicate.[22] Two

comparisons are of interest. First, the ν_1 (a_1) and ν_3 (b_2) modes for OZrO are higher by 182 and 200 cm^{-1} than these modes for OYO^-, respectively, and the differences increase to 227 and 255 cm^{-1} between OHfO and $OLaO^-$. Clearly, bonding is weaker in the isoelectronic anions. Moreover, large relativistic contraction[43] was found for Hf, and the frequencies of HfO and OHfO are within 1−2 cm^{-1} of the respective frequencies of ZrO and OZrO.[22] This relativistic contraction is clearly not observed for La as the LaO and OLaO frequencies are 46 and 138 cm^{-1} *lower* than the YO and OYO values, but this relativistic effect is observed for Ta,[38] which, like Hf, also follows the lanthanide series.

The $Y(O_2)^+$ and $La(O_2)^+$ cation reaction products are observed and enhanced by the addition of CCl_4 to serve as an electron trap.[27] Three stretching modes are predicted by BP86 calculations with different 16/18 isotopic ratios for symmetric O−O and Y−O_2 and antisymmetric Y−O_2 stretching modes with very good agreement both in frequency position and normal mode description as characterized by 16/18 isotopic frequency ratios.

The twenty frequencies observed here in solid argon and calculated by BP86/D95*/LanL2DZ provide both strong support for the identification of novel chemical species and a test for DFT frequency calculations. A recent reference gives scale factors for two pure density functionals (S-VWN and B-LYP) that are similar to BP86, the same basis sets employed here, and a set of frequencies including several first row transition metal compounds;[44] the relevant scale factors are 1.0057 and 1.0291. The present scale factors vary from 0.89 for the symmetric stretch of OLaO to 1.015 for the La−O fundamental. The O−O stretches of $Y(O_2)^+$ and $La(O_2)^+$ have essentially the same scale factor (0.938 and 0.935) as do (O_2)YO and (O_2)-LaO (0.986 and 0.980). The simple diatomic scale factors for YO (0.966) and YO^+ (0.943) are lower than values for LaO (1.015) and LaO^+ (1.014); these comparisons reveal complications from low energy configurations[21] not accounted for by DFT. The reverse is true for OYO (1.005) and OLaO (0.889), but these dioxides are very difficult theoretical subjects as described recently for OScO in studies contrasting DFT with higher levels of theory.[18,19] The OYO^- (0.981, 1.009) and $OLaO^-$ (1.002, 0.952) scale factors also vary in a nonsystematic fashion. Despite some variation, we conclude that low cost BP86 pseudopotential frequency calculations work extremely well as an aid to making vibrational assignments for Y and La oxide species. Using larger basis sets for O to include diffuse and polarization functions slightly reduces (1−19 cm^{-1}) the calculated frequencies and improves the fit; the calculated electron affinities and ionization energies for the diatomic molecules are within ±1 kcal/mol, but, for OYO and OLaO, calculated electron affinities increased about 10% while calculated ionization energies are within ±2 kcal/mol with the larger basis sets. Finally, the addition of an *f* polarization function on O and La gives further slight frequency decreases in most cases, but this minor improvement is probably not worth the effort.

Acknowledgment. We thank the National Science Foundation (CHE 97-00116) for financial support and the assistance of W. D. Bare with early experiments.

References and Notes

(1) Bednorz, J. G.; Muller, K. A.; Takashige, M. *Science* **1987**, *236*, 73.

(2) Aharoni, E.; Koren, G.; Oppenheim, U. P. *Physica C* ***1990***, *171*, 37. Kumar, D.; Apte, P. R.; Pinto, R. *J. Electrochem. Soc.* **1994**, *141*, 1611.

(3) Field, R. W. *Ber. Bunsen-Ges. Phys. Chem.* **1982**, *86*, 771.

(4) Chalek, C. L.; Gole, J. L. *J. Chem. Phys.* **1976**, *65*, 2845.

(5) Huber, K. P.; Herzberg, G. *Constants of Diatomic Molecules*, Van Nostrand Reinhold: New York, 1979.

(6) Steimle, T. C.; Al-Ramadin, Y. *J. Mol. Spectrosc.* **1987**, *122*, 103; Childs, W. J.; Poulsen, O.; Steimle, T. C. *J. Chem. Phys.* **1988**, *88*, 598.

(7) Törring, T.; Zimmermann, K.; Hoeft, J. *Chem. Phys. Lett.* **1988**, *151*, 520; Hoeft, J.; Törring, T. *Chem. Phys. Lett.* **1993**, *215*, 367.

(8) Suenram, R. D.; Lovas, F. Y.; Fraser, G. T.; Matsumura, K. *J. Chem. Phys.* **1990**, *92*, 4724.

(9) Simard, B.; James, A. M.; Hackett, P. A.; Balfour, W. J. *J. Mol. Spectrosc.* **1992**, *154*, 455.

(10) Behere, S. H.; Bhartiya, J. B. *J. Quant. Spectrosc. Radiat. Transfer* **1993**, *49*, 449.

(11) Fried, D.; Kushida, T.; Peck, G. P.; Rothe, E. W. *Appl. Spectrosc.* **1994**, *48*, 248.

(12) Carette, P.; Bencheikh, M. *J. Mol. Spectrosc.* **1994**, *163*, 309.

(13) Marquez, A.; Capitan, M. J.; Odriozola, J. A.; Sanz, J. F. *Intl. J. Quantum Chem.* **1994**, *52*, 1329.

(14) Weltner, W., Jr.; McLeod, D.; Kesai, P. H. *J. Chem. Phys.* **1967**, *44*, 3172.

(15) Howard, J. A.; Histed, M.; Mile, B.; Hampson, C. A.; Morris, H. *J. Chem. Soc., Faraday Trans.* **1991**, *87*, 3189.

(16) Clemmer, D. E.; Dalleska, N. F.; Armentrout, P. B. *Chem. Phys. Lett.* **1992**, *190*, 259.

(17) Chertihin, G. V.; Andrews, L.; Rosi, M.; Bauschlicher, C. W., Jr. *J. Phys. Chem. A* **1997**, *101*, 9085.

(18) Rosi, M.; Bauschlicher, C. W., Jr.; Chertihin, G. V.; Andrews, L. *Theor. Chem. Acc.* **1998**, *99*, 106.

(19) Bauschlicher, C. W., Jr.; Zhou, M. F.; Andrews, L.; Johnson, J. R. T.; Panas, I.; Snis, A.; Roos, B. O. *J. Phys. Chem. A* **1999**, *103*, 5463−5467.

(20) Wu, H.; Wang, L. S. *J. Phys. Chem. A* **1998**, *102*, 9129.

(21) Moore, C. E. *Atomic Energy Levels*, Circular 467; National Bureau of Standards: Washington, DC, 1949.

(22) Chertihin, G. V.; Andrews, L. *J. Phys. Chem.* **1995**, *99*, 6356 (TiO_2).

(23) Chertihin, G. V.; Bare, W. D.; Andrews, L. *J. Phys. Chem. A* **1997**, *101*, 5090 (VO_2).

(24) Chertihin, G. V.; Bare, W. D.; Andrews, L. *J. Chem. Phys.* **1997**, *107*, 2798 (CrO_2).

(25) Chertihin, G. V.; Andrews, L. *J. Phys. Chem. A* **1997**, *101*, 8547 (MnO_2).

(26) Chertihin, G. V.; Saffel, W.; Yustein, J. T.; Andrews, L.; Neurock, M.; Ricca, A.; Bauschlicher, C. W., Jr. *J. Phys. Chem.* **1996**, *100*, 5261 (FeO_2).

(27) Zhou, M. F.; Chertihin, G. V.; Andrews, L. *J. Chem. Phys.* **1998**, *109*, 10893 and references therein.

(28) Chertihin, G. V.; Andrews, L. *J. Chem. Phys.* **1998**, *108*, 6404.

(29) Zhou, M. F.; Hacaloglu, J.; Andrews, L. *J. Chem. Phys.* **1999**, *110*, 9450.

(30) Frisch, M. J.; Trucks, G. W.; Schlegel, H. B.; Gill, P. M. W.; Johnson, B. G.; Robb, M. A.; Cheeseman, J. R.; Keith, T.; Petersson, G. A.; Montgomery, J. A.; Raghavachari, K.; Al-Laham, M. A.; Zakrzewski, V. G.; Ortiz, J. V.; Foresman, J. B.; Cioslowski, J.; Stefanov, B. B.; Nanayakkara, A.; Challacombe, M.; Peng, C. Y.; Ayala, P. Y.; Chen, W.; Wong, M. W.; Andres, J. L.; Replogle, E. S.; Gomperts, R.; Martin, R. L.; Fox, D. J.; Binkley, J. S.; Defrees, D. J.; Baker, J.; Stewart, J. P.; Head-Gordon, M.; Gonzalez, C.; Pople, J. A. *Gaussian 94, Revision B.1* Gaussian, Inc.: Pittsburgh, PA, 1995.

(31) Lee, C.; Yang, E.; Parr, R. G. *Phys. Rev. B* **1988**, *37*, 785.

(32) Dunning, T. R., Jr.; Hay, P. J. in *Modern Theoretical Chemistry*; Schaefer, H. F., III, Ed.; Plenum: New York, 1976. Hehre, W. J.; Ditchfield, R.; Pople, J. A. *J. Chem. Phys.* **1972**, *56*, 2257. McLean, A. D.; Chandler, G. S. *J. Chem. Phys.* **1980**, *72*, 5639.

(33) Hay, P. J.; Wadt, W. R. *J. Chem. Phys.* **1985**, *82*, 299.

(34) Zhou, M. F.; Andrews, L. *J. Am. Chem. Soc.* **1998**, *120*, 13230.

(35) Allavena, M.; Rysnik, R.; White, D.; Calder, V.; Mann, D. E. *J. Chem. Phys.* **1969**, *50*, 3399.

(36) Andrews, L.; Yustein, J. T.; Thompson, C. A.; Hunt, R. D. *J. Chem. Phys.* **1994**, *98*, 6514.

(37) Darling, J. H.; Ogden, J. S. *J. Chem. Soc., Dalton Trans.* **1972**, 2496.

(38) Zhou, M. F.; Andrews, L. *J. Phys. Chem. A* **1998**, *102*, 8251.

(39) Chertihin, G. V.; Andrews, L.; Bauschlicher, C. W., Jr. *J. Phys. Chem. A* **1997**, *101*, 4026.

(40) Chertihin, G. V.; Andrews, L. *J. Chem. Phys.* **1997**, *106*, 3457.

(41) Citra, A.; Andrews, L. *J. Phys. Chem. A* **1999**, *103*, 4845.

(42) Willson, S. P.; Andrews, L. *J. Phys. Chem. A* **1999**, *103*, 3171.

(43) Pyykko, P. *Chem. Rev.* **1988**, *88*, 563.

(44) Bytheway, I.; Wong, M. W. *Chem. Phys. Lett.* **1988**, *282*, 219.